A POSTERIORI ERROR ESTIMATES FOR FINITE VOLUME ELEMENT APPROXIMATIONS OF CONVECTION-DIFFUSION-REACTION EQUATIONS

R.D. LAZAROV AND S.Z. TOMOV

ABSTRACT. We present the results of a study on a posteriori error control strategies for finite volume element approximations of second order elliptic differential equations. We adapt the local refinement techniques known from the finite element method to the finite volume discretizations of various boundary value problems for steady-state convection-diffusion-reaction equations. One possible application of such problems is simulation of fluid flow and transport of passive chemicals in porous media. Locally conservative approximation schemes and methods with a posteriori error control play important role for such problems. Finite volume methods ensure local mass conservation and combined with some upwind strategies give monotone solutions. In this paper we present an analysis of a residual type error estimators and illustrate our theoretical findings on numerous computational tests in 2 and 3 dimensions.

1. Introduction

We consider the following convection-diffusion-reaction problem: Find $u = u(x)$ such that

$$(1.1)\qquad \begin{cases} Lu \equiv -\nabla \cdot A\nabla u + \nabla \cdot (\underline{b}u) + cu &= f, \qquad \text{in } \Omega, \\ u &= 0, \qquad \text{on } \Gamma_D, \\ (-A\nabla u + \underline{b}u)\cdot \underline{n} &= g_N, \qquad \text{on } \Gamma_N^{in}, \\ -A\nabla u \cdot \underline{n} &= 0, \qquad \text{on } \Gamma_N^{out}. \end{cases}$$

Here Ω is a bounded polygonal domain in R^n, $n = 2, 3$, $A = A(x)$ is $n \times n$ symmetric, bounded and uniformly positive definite matrix in Ω, $\underline{n}$ is unit vector pointing outward and normal to Γ, $\underline{b} = \underline{b}(x) = (b_1(x), \dots, b_n(x))$ is a given vector function, $c = c(x)$ is the given absorption/reaction coefficient, and $f = f(x)$ is a given source function. We have also used the notation ∇u for the gradient of a scalar function u and $\nabla \cdot \underline{b}$ for the divergence of a vector function $\underline{b}$ in R^n. The boundary of Ω, Γ, is split into

Date: August 8, 2001.

1991 *Mathematics Subject Classification.* 65N30, 65M35.

Key words and phrases. convection-diffusion-reaction equations, finite volume approximation, a posterior error estimators, residual estimators, ZZ-patch test.

This work has been partially supported by the US National Science Foundation under grant DMS–9973328. Part of the work has been supported by DOE-LLNL through the summer visits of the authors to the University of California Lawrence Livermore National Laboratory.

Dirichlet Γ_D and Neumann Γ_N parts. Further, the Neumann boundary is divided into two parts: $\Gamma_N = \Gamma_N^{in} \cup \Gamma_N^{out}$, where $\Gamma_N^{in} = \{x \in \Gamma_N : \underline{n}(x) \cdot \underline{b}(x) < 0\}$ and $\Gamma_N^{out} = \{x \in \Gamma_N : \underline{n}(x) \cdot \underline{b}(x) \geq 0\}$. We assume that Γ_D is a nonempty and has positive measure.

This model problem comes from simulation of fluid flow and transport in porous media. For example, $u(x)$ may represent the concentration of a chemical dissolved and distributed in water due to processes of advection, diffusion, and absorption. The solution of such problems exhibit local behavior due to discontinuity in the boundary data and the coefficients of the differential equations, and/or other local phenomena (for example extraction/injection wells). In order to resolve such local behavior the numerical method should be able to detect the regions of singular behavior of the solution and to refine the grid locally in a balanced manner, so that the overall accuracy is uniform in the whole domain. The local conservation properties of the finite volume element approximations and the simplicity of the method motivated our study.

There are few works related to a posteriori error estimates for finite volume methods. In the pioneering work [1] L. Angermann has studied a balanced a posteriori error estimates for finite volume discretizations for convection-diffusion equations in 2-D on Voronoi meshes. His basic error estimator is derived using the idea of a previous work [2] on finite element method but contains two new terms which he has studied. In our paper we take a similar path. Namely, the error estimates for the finite volume method are derived by using the relation and similarities between the finite volume and finite element methods. The theory of the finite volume methods is still under development and this raises the difficulties in establishing an independent a posteriori error analysis for finite volume approximations. For instance, optimal order a-priori L^2-error estimates with minimal regularity of the solution are not known for the finite volume methods for elliptic equations. Optimal $W^{1,p}$-error estimates for elliptic and parabolic problems have been obtained in the recent studies [16, 19] for $1 < p \leq \infty$.

On the other hand, a posteriori error indicators and estimators for the finite element method have been widely used and studied in the past 25 years. The research in this area starts with the pioneering papers of Babuska and Rheinboldt [4] and continues with studies devoted to the so called *Residual Based* method (see the survey paper of Verfürth [27]). In this popular approach certain local residuals are evaluated and then the a posteriori error indicator is obtained by solving local Dirichlet or Neumann problems taking the residuals as data [4, 5]. Another variation of the method is to use the Galerkin orthogonality, a priori interpolation estimates and global stability in order to get error estimators in global L^2- and H^1-norms (see, for example, [14]). Further, solving appropriate dual problems, instead of using the a priori interpolation estimates, leads to error estimators controlling various kinds of error functionals [6]. Solving finite element problems in an enriched by hierarchical bases function space gives rise to the so called *Hierarchical Based* error estimators [5]. There are error estimators that control the error or its gradient in the maximum norm. Such estimators are based on optimal a priori estimates for the error in maximum norm [15]. Another error indicator, which is widely (and in most cases heuristically) used in many adaptive finite element codes, is the *Zienkiewicz-Zhu* (often called *ZZ*) error estimator [29, 30]. This estimator is based on post-processing of the computed solution gradient in order to get a better one, which is later used instead of the exact gradient to estimate the energy norm of the error. Some analysis of the method could be found in [21] and the literature cited there.

In this paper we adapt the mentioned above finite element local error estimation techniques to the case of finite volume element approximations. We consider mainly the *Residual Based* a-posteriori error estimators and analyze exclusively the one that controls the error in global L^2- and H^1-norms and uses Galerkin orthogonality, a priori interpolation estimates and global stability. Our theoretical and experimental findings are similar to those in [1] and could be summarized as follows: the a posteriori error estimates in the finite volume element method are quite close to those in the finite element method and the mathematical tools from the finite element theory can be successfully applied for their analysis.

The paper is organized as follows. We start with the finite volume element formulation in Section 2. The section defines the used notations, approximations and gives some general results from the finite volume approximations. Next section studies the *Residual Based* error estimator, followed by short explanation of Zienkiewicz-Zhu estimator in Section 4. In Section 5 we summarize the used adaptive refinement strategy. Finally, various computational results for model 2 and 3 dimensional problems, confirming our theoretical findings are given in Section 6.

2. Finite volume element formulation

2.1. **Notations.** We use the Hilbert space $H^1_D(\Omega) = \{v \in H^1(\Omega) : \ v|_{\Gamma_D} = 0\}$ and the standard L^2- and H^1-norms:

$$||u|| = (u,u)^{1/2}, \ ||u||_{1,\Omega} \equiv ||u||_1 = \{(u,u) + (\nabla u, \nabla u)\}^{1/2},$$

where $(\cdot,\cdot)$ is the inner product in $L^2(\Omega)$ and ∇u is the gradient of u.

We shall use the weak formulation of the problem (1.1). First we introduce the bilinear from $a(\cdot,\cdot)$, defined on $H^1_D(\Omega) \times H^1_D(\Omega)$ as:

$$a(u,v) \equiv (A\nabla u - \underline{b}u, \nabla v) + (cu, v) + \int_{\Gamma_N^{out}} \underline{b}\cdot\underline{n}\ u\ vds. \tag{2.2}$$

We assume that the coefficients of problem (1.1) satisfy the following conditions:
(a) the form is coercive in $H^1_D(\Omega)$, i.e. there is a constant $c_0 > 0$ s.t.

$$a(u,u) \geq c_0||u||_1^2, \ \forall u \in H^1_D(\Omega);$$

(b) the form is bounded in $H^1_D(\Omega)$, i.e. there is a constant $c_1 > 0$ s.t.

$$a(u,v) \leq c_1||u||_1||v||_1, \ \forall u, \ v \in H^1_D(\Omega).$$

A sufficient condition for the coercivity of the bilinear form is

$$c(x) + 0.5\nabla \cdot \underline{b}(x) \geq 0 \quad \text{for all } x \in \Omega.$$

Then (1.1) has the following weak form: Find $u \in H_D^1(\Omega)$ such that

$$a(u, v) = (F, v) \equiv (f, v) - \int_{\Gamma_N^{in}} g_N v ds \text{ for all } v \in H_D^1(\Omega). \tag{2.3}$$

In pur computations we also use the standard energy norm $||u||_a^2 = a(u, u)$. Finally, when we derive a posteriori error estimates in L^2-norm we shall assume that problem (2.3) is H^2-regular, i.e. the solution is in $H^2(\Omega) \cap H_D^1(\Omega)$.

2.2. **Approximation method.** We assume that Ω is a convex polygonal domain and is partitioned into triangles (in 2-D) or tetrahedra (in 3-D) called finite elements and denoted by K. The elements are considered to be closed sets and the splitting is denoted by $\mathcal{T}_h$. We assume that the partition $\mathcal{T}_h$ is locally quasi-uniform (or regular), that is meas$(K) \leq C\rho(K)^d$ with a constant independent of the partiton. Here $\rho(K)$ is the radius of the largest ball contained in K. In the context of locally refined grids this means that neigbouring finite elements are of approximately the same size while elements that are far away may have very different size.

We introduce the set $N_h = \{p : p \text{ is a vertex of element } K \in \mathcal{T}_h\}$ and define N_h^0 as the set of all vertices from N_h except those on Γ_D. For a given vertex x_i we denote by $\Pi(i)$ the index set of all neighbors of x_i in N_h, i.e. all vertices that are connected to x_i by an edge.

In order to derive the finite volume approximation we need the so-called dual partitioning of Ω into finite volumes. For a given finite element partitioning $\mathcal{T}_h$, we construct a dual mesh $\mathcal{T}_h^*$ (based upon $\mathcal{T}_h$), whose elements are called control volumes. In the finite volume methods there are various ways to introduce the control volumes. Almost all approaches can be described in the following general scheme. In each element $K \in \mathcal{T}_h$ a point q is selected. For the 3-D case, on each of the four faces $\overline{x_i x_j x_k}$ of K a point x_{ijk} is selected and on each of the six edges $\overline{x_i x_j}$ a point x_{ij} is selected. Then q is connected to the points x_{ijk}, and in the corresponding faces the points x_{ijk} are connected to the points x_{ij} by straight lines (see Figure 1). The control volumes are associated to the vertices $x_i \in N_h$. Control volume associated with vertex x_i is denoted by V_i and defined as the union of the "quarter" elements $K \in \mathcal{T}_h$, which have x_i as a vertex (see Figure 1). The interface between two control volumes, V_i and V_j, is denoted by γ_{ij}.

We assume that the partitioning $\mathcal{T}_h^*$ is locally quasi-uniform (or regular) in R^n, $n = 2, 3$. This means that there exists a positive constant $C > 0$ such that $C^{-1}h_i^n \leq$ meas$(V_i) \leq Ch_i^n$, for all $V_i \in \mathcal{T}_h^*$. Here h_i is the maximal diameter of the elements $K \in \mathcal{T}_h$ that intersect V_i.

For the 2-D case we will also use the construction of the control volumes in which the point q is the circumcenter of the element K, i.e. the center of the circumscribed circle of K and x_{ij} are the midpoints of the edges of K. This type of control volume forms

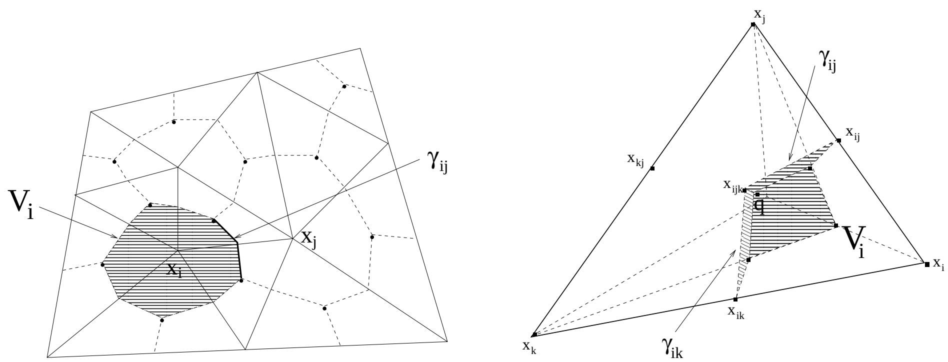

FIGURE 1. Left: Finite element and finite volume partitions in 2-D; Right: Contribution from one element to control volume V_i, γ_{ij} and γ_{ik} in 3-D; Point q is the element's medicenter and internal points for the faces are the medicenters of the faces.

the so-called Voronoi meshes. Then obviously, γ_{ij} are the perpendicular bisectors of the three edges of K (see Figure 2). This construction requires that all finite elements are triangles of acute type, which we shall assume whenever such triangulation is used.

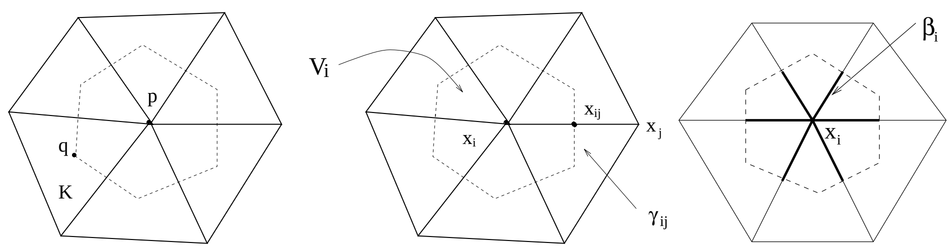

FIGURE 2. Control volumes with circumcenters as internal points (Voronoi meshes) and interface γ_{ij} of V_i and V_j. The rightmost picture shows the segments β_i in bold.

We define the linear finite element space S_h as

$$S_h = \{v \in C(\Omega) : \ \ v|_K \text{ is linear for all } \ K \in \mathcal{T}_h \text{ and } v|_{\Gamma_D} = 0\}$$

and its dual volume element space S_h^* by

$$S_h^* = \{v \in L^2(\Omega) : \ \ v|_V \text{ is constant for all } \ V \in \mathcal{T}_h^* \text{ and } v|_{\Gamma_D} = 0\}.$$

Obviously, $S_h = \text{span}\{\phi_i(x) : \ x_i \in N_h^0\}$ and S_h^* =span$\{\chi_i(x) : \ x_i \in N_h^0\}$, where ϕ_i are the standard nodal linear basis functions associated with the node x_i and χ_i are the characteristic functions of the volume V_i. Let $I_h : C(\Omega) \to S_h$ be the interpolation operator and $I_h^* : C(\Omega) \to S_h^*$ and $P_h^* : C(\Omega) \to S_h^*$ be the piece-wise constant interpolation and projection operators, respectively. That is

$$I_h u = \sum_{x_i \in N_h} u(x_i)\phi_i(x), \ \ I_h^* u = \sum_{x_i \in N_h} u(x_i)\chi_i(x), \ \text{ and } P_h^* u = \sum_{x_i \in N_h} \bar{u}_i \chi_i(x).$$

Here, $\bar{u}_i$ is the averaged value of u over the volume V_i. i.e. $\bar{u}_i = \int_{V_i} u\,dx/|V_i|$. In fact I_h makes also sense as an interpolation operator from S_h^* to S_h, namely $I_h v^* \in S_h$ and $I_h v^*(x_i) = v^*(x_i)$.

The finite volume element approximation u_h of (1.1) is the solution to the problem: Find $u_h \in S_h$ such that

$$a_h(u_h, v^*) \equiv A(u_h, v^*) + C(u_h, v^*) = F(v^*), \text{ for all } v^* \in S_h^*. \tag{2.4}$$

Here the bilinear forms $A(u_h, v^*)$ and $C(u_h, v^*)$ are defined on $S_h \times S_h^*$, the linear form $F(v^*)$ on S_h^*, and are given by

$$A(u_h, v^*) = \sum_{x_i \in N_h^0} v_i^* \left\{ - \int\limits_{\partial V_i \setminus \Gamma_N} A\nabla u_h \cdot \underline{n} ds + \int\limits_{V_i} c u_h dx \right\}, \tag{2.5}$$

$$F(v^*) = \sum_{x_i \in N_h^0} v_i^* \left\{ \int\limits_{V_i} f dx - \int\limits_{\partial V_i \cap \Gamma_N^{in}} g_N ds \right\}. \tag{2.6}$$

Here and further we use the notation $v_i^* = v^*(x_i)$. We use two different approximations for computing $C(u_h, v^*)$. The first one is a straightforward evaluation of $C(u_h, v^*)$:

$$C(u_h, v^*) = \sum_{x_i \in N_h^0} v_i^* \int\limits_{\partial V_i \setminus \Gamma_N^{in}} \underline{b} \cdot \underline{n} u_h ds, \; u_h \in S_h, \; v^* \in S_h^*. \tag{2.7}$$

Such approximation can be used for moderate convection fields and dominating diffusion. For large convection (or small diffusion) this approximation gives oscillating numerical results which we would like to avoid. For such problems we are interested in approximation methods that produce solutions satisfying the maximum principle and are locally conservative. Such schemes are also known as monotone schemes (see, e.g. [17, 22]). A well-known sufficient condition for a scheme to be monotone is that the corresponding stiffness matrix is an M–matrix.

The up-wind approximation of convection-dominated problems, which we have used here, is locally mass conservative and gives the desired stabilization. It is done in the following way. We split the integral over ∂V_i on integrals over $\gamma_{ij} = \partial V_i \cap \partial V_j$, (see Figure 1) and introduce outflow and inflow parts of the boundary of the volume V_i. This splitting can be characterized by the quantities $(\underline{b} \cdot \underline{n}_i)_+ = \max(0, \; \underline{b} \cdot \underline{n}_i)$ and $(\underline{b} \cdot \underline{n}_i)_- = \min(0, \; \underline{b} \cdot \underline{n}_i)$, where $\underline{n}_i$ is the outer unit vector normal to ∂V_i. Then the convection form $C(u_h, v^*)$ is defined as

$$C(u_h, v^*) = \sum_{x_i \in N_h^0} v_i^* \sum_{j \in \Pi(i)} \int\limits_{\gamma_{ij}} \left[(\underline{b} \cdot \underline{n}_i)_+ u_h(x_i) + (\underline{b} \cdot \underline{n}_i)_- u_h(x_j) \right] \, ds. \tag{2.8}$$

This is an extension of the classical upwind approximation of the convection term and is closely related to the discontinuous Galerkin approximation or to the Tabata scheme for Galerkin finite element method [24]. It is also related to the scheme on Voronoi meshes derived by Mishev in [20]. A different type of weighted upwind approximation on Voronoi meshes in 2-D has been studied in [1].

We recall the following result from the finite volume element approximations [10, 11, 16, 19]. Let u and u_h be the exact solution of (1.1) and the finite volume element approximation (2.4), respectively. Then there is an independent of h constant $C > 0$ such that

$$||u - u_h||_1 \le Ch||u||_2. \tag{2.9}$$

3. The residual type error estimators

Since $u_h \in S_h \subset H^1_D(\Omega)$ the problem of finding the exact error $e = u - u_h$ has the following weak formulation : Find $e \in H^1_D(\Omega)$ such that

$$a(e, v) = (F, v) - a(u_h, v) \equiv (R, v) \quad \text{for all} \quad v \in H^1_D(\Omega). \tag{3.10}$$

Most of the residual type error estimators try to solve (3.10) in an enriched finite dimensional space S, $S_h \subset S \subset H^1_D(\Omega)$, which is usually obtained by adaptively refining the grid $\mathcal{T}_h$ (the so called h-refinement) or by increasing the order of the algebraic polynomials used in the approximation process (the so called p-refinement). Such global solution technique is computationally expensive and is usually replaced by solving the problem locally. The h-refinement is used in subsection (3.3) to define residual based error estimators as solutions of local Dirichlet or Neumann problems.

Computationally less expensive is another approach based on computing certain local residuals (over the elements $K \in \mathcal{T}_h$) and using: (1) the Galerkin orthogonality $a(e, e) = (R, e - e_h)$ for any $e_h \in S^*_h$, (2) the a priori interpolation estimates for $e - e_h$, locally on the elements, and (3) the global stability estimate. Such approach gives rise to an error estimator in the global H^1-norm, described in subsection 3.1. Using duality one can get error estimators in the L^2-norm or error estimators that control different types of error functionals (see for more details Subsection 3.2).

3.1. **Error estimators based on Local Residuals.** This method expresses the error as sum of certain local residuals over the elements. These local residuals are in terms of the difference of the exact and approximate solution over the elements and the jumps of the conormal derivatives along the element faces/edges for the 3-D/2-D case.

We first demonstrate the method when **no upwind** is used for the approximation of the convection term, i.e. the form $C(\cdot, \cdot)$ is evaluated by (2.7). In this case $a_h(\cdot, v^*) = a(\cdot, v^*)$. We give a posteriori estimate for the error $e = u - u_h$, where u is the solution of the weak problem (2.3). Using the divergence theorem over the volumes and regrouping the sum over the volumes as sum over the elements we get:

$$\begin{aligned} a(e,v^*) &= \sum_{x_i \in N_h^0} v_i^* \left\{ \int_{V_i} (f + \nabla\cdot(A\nabla u_h - \underline{b}u_h) - cu_h)\,dx - \int_{\beta_i\setminus\Gamma_N} [A\nabla u_h]\cdot\underline{n}ds \right. \\ &\qquad \left. - \int_{\beta_i\cap\Gamma_N^{in}} g_N + (A\nabla u_h - \underline{b}u_h)\cdot\underline{n}ds - \int_{\beta_i\cap\Gamma_N^{out}} A\nabla u_h\cdot\underline{n}ds \right\} \\ &= \sum_{K\in\mathcal{T}_h} \left\{ \int_K (f + \nabla\cdot A\nabla u_h - \nabla\cdot(\underline{b}u_h) - cu_h)v^*dx - \frac{1}{2}\int_{\partial K\setminus\Gamma_N} [A\nabla u_h]\cdot\underline{n}v^*ds \right. \\ &\qquad \left. - \int_{\partial K\cap\Gamma_N^{in}} (g_N + (A\nabla u_h - \underline{b}u_h)\cdot\underline{n})v^*ds - \int_{\partial K\cap\Gamma_N^{out}} (A\nabla u_h\cdot\underline{n})v^*ds \right\} \\ &\equiv \sum_{K\in\mathcal{T}_h} \{(R_K,v^*)_K + (R_{\partial K},v^*)_{\partial K}\} \quad for\ all \quad v^*\in S_h^*. \end{aligned}$$

Here $[A\nabla u_h]$ denotes the jump of $A\nabla u_h$ across the finite element boundary and β_i is defined as $\beta_i \equiv V_i \cap \sum_{K\in\mathcal{T}_h}\partial K$ (see Figure 2 for the 2-D case). The last equality defines R_K as the residual over the element K and $R_{\partial K}$ as the jump across the element boundary. Using the weak formulation given by (2.3), integrating by parts, we get similar expression for e as well:

$$a(e,v) = \sum_{K\in\mathcal{T}_h} \{(R_K,v)_K + (R_{\partial K},v)_{\partial K}\} \text{ for all } v\in H_D^1(\Omega).$$

Here we have grouped all boundary terms to define $R_{\partial K}$ and all terms with integration over finite elements K to define R_K.

In what follows, the second argument of the bilinear form $a(\cdot,\cdot)$ will determine whether it is the bilinear form for finite volumes, $a(\cdot,v^*)$, or the bilinear form for finite elements, $a(\cdot,v)$. Using the Petrov-Galerkin orthogonality for the finite volume method $a(e,v^*)=0$, for all $v^*\in S_h^*$, and applying Hölder's inequality on each element leads to the following estimate for the error in the energy norm:

$$\begin{aligned} c_0||e||_1^2 &\le a(e,e) = a(e,e) - a(e,v^*) \\ &= \sum_{K\in\mathcal{T}_h} \{(R_K,e-v^*)_K + (R_{\partial K},e-v^*)_{\partial K}\} \le \sum_{K\in\mathcal{T}_h} \rho_K\omega_K(e). \end{aligned} \tag{3.11}$$

Here the local residuals ρ_K and the weights ω_K are defined by

$$\rho_K := h_K||R_K||_K + h_K^{1/2}||R_{\partial K}||_{\partial K}, \tag{3.12}$$

$$\omega_K(e) := max\left\{h_K^{-1}||e-v^*||_K, h_K^{-1/2}||e-v^*||_{\partial K}\right\}. \tag{3.13}$$

Here v^* is an arbitrary element in S_h^*. Note that with the introduced notations inequality (3.11) can be written also in the following form, which will be used later:

$$a(e,v) \le \sum_{K\in\mathcal{T}_h} \rho_K \omega_K(v) \ \text{ for all } \ v \in H_D^1(\Omega).$$

Further, one should use the local approximation properties of the space S_h^* in order to estimate $\omega_K(e)$. Namely, we use the concept of quasi interpolation (see, e.g. [8, 12, 13]) and we proceed as follows. Let $\pi(K)$ be a patch of all finite elements that share a vertex with K. Using the local L^2-projection (see [8], formula (3.2)) one can find $v(e) \in S_h$ such that

$$h_K^{-1}||e - v(e)||_K + h_K^{-1/2}||e - v(e)||_{\partial K} + ||\nabla v(e)||_K \le C_{I,K}||\nabla e||_{\pi(K)}.$$

Then taking $v^* = I_h^* v(e)$ in (3.13), using the above estimate, inequality (3.11) and obvious manipulations, we get

$$||e||_1 \le CC_I \left(\sum_{K\in\mathcal{T}_h} \rho_K^2 \right)^{1/2},$$

where C depends on the coercivity constant c_0 of the form $a(\cdot,\cdot)$ and $C_I = \max_{K\in\mathcal{T}_h} C_{I,K}$.

Next, we study the case of **up-wind** approximation. In this case $a_h(\cdot,\cdot)$ is defined by (2.4) and the convection part is determined by (2.8). The up-wind approximation of the convection will bring additional error term and we modify the above argument in the following way. From $a_h(u_h, v^*) = F(v^*)$ and $a(u,v^*) = F(v^*)$ for $v^* \in S_h^*$ we get the orthogonality condition:

$$a(u,v^*) - a_h(u_h, v^*) = 0.$$

Following (3.11), the estimate for the error in the energy norm now becomes

$$\begin{aligned} c_0||e||_1^2 &\le a(e,e) = a(e,e) - a(u,v^*) + a_h(u_h,v^*) \\ &= \{a(e,e) - a(e,v^*)\} + \{a_h(u_h,v^*) - a(u_h,v^*)\}. \end{aligned}$$

To estimates the term $a(e,e) - a(e,v^*)$ we use (3.11). For the second term, $a_h(u_h,v^*) - a(u_h,v^*)$, we get

$$\begin{aligned} a_h(u_h,v^*) - a(u_h,v^*) &= \sum_{x_i\in N_h^0} v_i^* \int_{\partial V_i} \left[(\underline{b}\cdot\underline{n}_i)_+ u_h(x_i) + (\underline{b}\cdot\underline{n}_i)_- u_h(x_j) - \underline{b}\cdot\underline{n}_i u_h\right] \, ds \\ &= \sum_{K\in\mathcal{T}_h} \sum_{\gamma_{ij}\subset K} (v_i^* - v_j^*) \int_{\gamma_{ij}} \underline{b}\cdot\underline{n}(u_h(x_i) - u_h) ds. \end{aligned}$$

In the last equality $\underline{n}$ is taken to be the normal to γ_{ij} such that $\underline{b}\cdot\underline{n} \ge 0$ and the indices (ij) are such that $(x_i - x_j)\cdot\underline{n} \le 0$. We denote by $[v^*]$ the jump of v^* across γ_{ij} and by $R_{\gamma_{ij}}$ the expression $\underline{b} \cdot \underline{n}(u_h(x_i) - u_h)|_{\gamma_{ij}}$. Then, by Schwartz inequality, we get the bound

$$a_h(u_h, v^*) - a(u_h, v^*) \leq \sum_{K \in \mathcal{T}_h} \sum_{\gamma_{ij} \subset K} ||[e - v^*]||_{\gamma_{ij}} ||R_{\gamma_{ij}}||_{\gamma_{ij}} \leq \sum_{K \in \mathcal{T}_h} \omega_K^\gamma \; h_K^{1/2} ||R_{\gamma_K}||.$$

Here $|| \cdot ||_{\gamma_{ij}}$ denotes the L^2-norm on γ_{ij} and in the last inequality we have used the notations

$$\omega_K^\gamma = h_K^{-1/2} \left(\sum_{\gamma_{ij} \subset K} ||[e - v^*]||^2_{\gamma_{ij}} \right)^{1/2}, \; ||R_{\gamma_K}|| = \left(\sum_{\gamma_{ij} \subset K} ||R_{\gamma_{ij}}||^2_{\gamma_{ij}} \right)^{1/2}.$$

Again, by using the local quasi interpolant and its approximation properties we get $\sum_{K \in \in \mathcal{T}_h} \omega_K^\gamma \leq C_I ||\nabla e||_\Omega$. This means that we have to add to the local residuals ρ_K additional term $h_K^{1/2} ||R_{\gamma_K}||$, i.e.

$$\rho_K := h_K ||R_K||_K + h_K^{1/2} ||R_{\partial K}||_{\partial K} + h_K^{1/2} ||R_{\gamma_K}||,$$

and proceed further as in the previous case.

The obtained through inequality (3.11) a posteriori error estimator is similar to the one from the finite element method. One may further exploit the similarity of the error estimates for finite elements and finite volumes. We shall use this similarity to derive an a posteriori error estimate in L^2-norm by using duality argument.

Let us denote by e^{FE} the error in the corresponding finite element method (using linear triangles). Then one gets the formula

$$c_0 ||e^{FE}||_1^2 \leq \sum_{K \in \mathcal{T}_h} \{ (R_K, e^{FE} - v)_K + (R_{\partial K}, e^{FE} - v)_{\partial K} \} \leq \sum_{K \in \mathcal{T}_h} \rho_K \omega_K(e^{FE}),$$

i.e. the weights $\omega_K(e^{FE})$ in the finite element method are defined as in (3.13) but with $v^* \in S_h^*$ replaced by $v \in S_h$. To get error estimate in L^2-norm, as given in subsection 3.2, one considers the dual problem : Find $\tilde{e} \in H_D^1(\Omega)$ such that

$$a(v, \tilde{e}) = (e^{FE}, v) \text{ for any } v \in H_D^1(\Omega).$$

Thus $||e^{FE}||_0^2 = a(e^{FE}, \tilde{e}) \leq \sum\limits_{K \in \mathcal{T}_h} \rho_K \omega_K(\tilde{e})$. For u sufficiently smooth, one can use interpolation estimate $\omega_K(\tilde{e}) \leq C_{I,K} h_K |\tilde{e}|_{2,K}$ (see, e.g. [9]) to finally get

$$||e^{FE}||_0 \leq C \left(\sum_{K \in \mathcal{T}_h} h_K^2 \rho_K^2 \right)^{1/2},$$

where C is the constant from the stability estimate for the dual problem $|\tilde{e}|_2 \leq C||e^{FE}||_0$. This shows that ρ_K can be used to get an a poteriori estimate for the error in L^2-norm.

We can use similar analysis to show that for problems with smooth data and solutions the derived estimator for the finite volume method produces asymptotically the same result. If $A(x)$ is piecewise constant matrix over the finite elements, then one can easily prove that $(R_{\partial K}, e - v^*)_{\partial K} = (R_{\partial K}, e - I_h v^*)_{\partial K}$ for any $v^* \in S_h^*$. Thus, the difference in the presentation of the errors of the finite element and finite volume methods is in the residual terms. To compare the residual terms one can proceed as follows. Denote by $P_K v \equiv \frac{1}{|K|}\int_K v dx$ and consequently get the following estimate for the finite volume error:

$$\begin{aligned}(R_K, e - v^*)_K &= (R_K - P_K R_K, e - v^*)_K + (P_K R_K, e - I_h v^*)_K \\ &\leq C_{I,K}\ h_K^2\ (||\nabla R_K||_K\ ||\nabla e||_K\ + ||R_K||_K\ |e|_{2,K}).\end{aligned}$$

Obviously, this term is of the same order as the corresponding term in the finite element case.

3.2. **Residual estimators using duality.** The asymptotic exactness of the above error estimator can be lost when applying the Hölder's inequality in (3.11). For example, this is the case for problems with strongly varying coefficients, convection dominated problems, etc. Also, the estimator may not be appropriate for controlling local quantities of the error (point values, line integrals, etc.). Such deficiency is inherited for almost all *Residual Based* error indicators based on local computations and is due to the fact that they do not control the error propagation or do it partially, of course for reasons of computational efficiency. The sharpness of the error estimates could be improved and the question is how much one is willing to spend on the computations in order to find the exact error.

In the residual method based on duality one increases the sharpness of the error estimators (which may be designed for different quantities of the error) by solving dual problems for the quantity of interest and using the obtained solution to compute better weighting factors ω_K in (3.11). The general idea is as follows. Consider the dual problem: Find $\tilde{e} \in H_0^1(\Omega)$ such that

$$a(v, \tilde{e}) = J(v) \text{ for any } v \in H_D^1(\Omega) \cap C^0(\bar{\Omega}),$$

where $J(\cdot)$ is linear error functional defined on $H_D^1(\Omega) \cap C^0(\bar{\Omega})$. For example, if one wants to control the error at point x, $J(v) = v(x)$ etc. Taking into the above equation $v = e$ and using the same approach as in (3.11) we get $|J(e)| \leq \sum_{K \in \mathcal{T}_h} \rho_K \omega_K(\tilde{e})$. The easiest way to estimate the weights $w_K(\tilde{e})$ is to use one of the a priori error estimates

$$\omega_K(\tilde{e}) \approx C_{I,K}||\nabla\tilde{e}||_K,\ \omega_K(\tilde{e}) \approx C_{I,K} h_K ||\tilde{e}||_{2,K}.$$

The second approxiame equality is valid is under certain assumptions, discussed in subsection (3.1).

Improvements, which of course lead to another increase in the computational cost, deal with techniques for direct evaluation of the residual in (3.11) (the quantity before applying Hölder's inequality). For more details we refer to [6].

3.3. **Estimators based on local Dirichlet/Neumann problems.** The error estimators in this subsection are obtained by replacing the expensive solution in an enriched finite dimensional space S, $S_h \subset S \subset H_D^1(\Omega)$, by solutions of local Dirichlet or Neumann problems. In the finite element setting S is usually obtained by using higher order polynomials over the same mesh (often called p-refinement, see [4, 5, 27] and next section). Here we obtain S by h-refinement and the definition of the local problems is as follows.

First, given a vertex x_i, we define K_i to be the union of all finite elements K that share x_i. We define $T_\delta(V_i)$ and $T_\delta(K_i)$ by splitting correspondingly V_i and K_i into finite elements of size $\delta \approx h/2$ in the way shown on Figure 3, and over the splitting define the finite element spaces

$$\begin{aligned} S_\delta(V_i) &= \{v \in C(\Omega): \ v|_K \text{ is linear for all } \ K \in T_\delta(V_i)\ \} \\ S_\delta(K_i) &= \{v \in C(\Omega): \ v|_K \text{ is linear for all } \ K \in T_\delta(K_i) \text{ and } v|_{\partial K_i} = 0\}, \end{aligned}$$

and their dual finite volume element spaces $S^*_\delta(V_i)$ and $S^*_\delta(K_i)$.

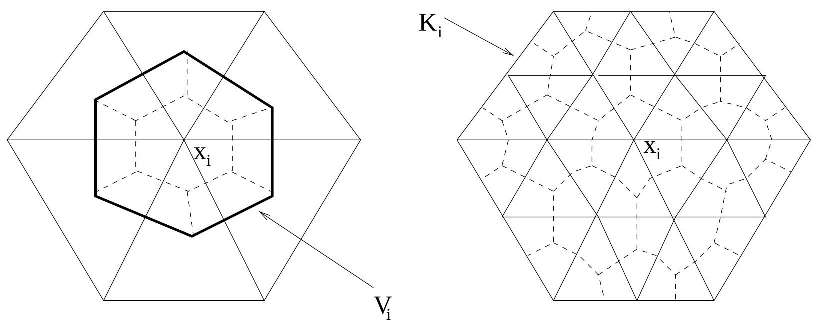

FIGURE 3. Local partitioning of V_i and K_i for the local Neumann and Dirichlet problems

The local Neumann problem, associated to volume V_i, is defined as : Find $u_\delta \in S_\delta(V_i)$ such that

$$A(u_\delta, v^*) + C(u_\delta, v^*) = F(v^*) \text{ for all } v^* \in S^*_\delta(V_i),$$

where the forms A, C and F are defined by (2.5), (2.7) and (2.6) with $\nabla u_\delta|_{\partial V_i} = \nabla u_h$.

The local Dirichlet problem, associated to K_i, is defined as : Find $u_\delta \in S_\delta(K_i)$ such that

$$A(u_\delta, v^*) + C(u_\delta, v^*) = F(v^*) \text{ for all } v^* \in S^*_\delta(K_i),$$

where the forms A, C and F are defined by (2.5), (2.7) and (2.6) with $u_\delta|_{\partial K_i} = u_h$.

The error estimators are defined for any vertex $x_i \in N_h$ as

$$\rho^N_{V_i} = ||\nabla u^N_\delta - \nabla u_h||_{V_i}, \text{ and } \rho^D_{K_i} = ||\nabla u^D_\delta - \nabla u_h||_{K_i},$$

where u^N_δ and u^D_δ are correspondingly the solutions to the local Neumann and Dirichlet problem.

Improvement of the error estimation for the cost of computational efficiency can be achieved by increasing the patches over which the local problems are defined and/or by performing properly defined iterative correction steps.

4. Zienkiewicz-Zhu (ZZ) estimator

Here we briefly describe another estimator that has been implemented and tested in our computations, namely *Zienkiewicz-Zhu (or ZZ) error estimator*, see [29]. This estimator is difficult to justify for convection-diffusion equations. We use it heuristically (as an error indicator). It's efficiency for various elliptic problems has been numerically confirmed in many practical applications (see for example the references in the survey paper [30]). Theoretical work on the method can be found for example in [21] and the literature cited therein. The estimator is also very easy to compute, making it very appealing for implementation in the adaptive mesh refinement software.

The ZZ indicator expresses the energy norm of the error $|||e||| \equiv (A\nabla e, \nabla e)$ through an approximation of the exact error gradient $\nabla e = \nabla(u - u_h)$. The computed gradient ∇u_h is post-processed expecting to get a better approximation ∇u_h^* for ∇u_h, which approximation is later substituted instead of the exact gradient ∇u into the error estimator $|||e|||$. This is done in the following way. We define the diffusive flux $\sigma \equiv -A\nabla u$. Then the finite element approximation for σ is given by $\sigma_h = -A\nabla u_h$ and the error for this approximation is denoted by $e_\sigma = \sigma - \sigma_h$. The error is considered in the $|||\ .\ |||$-norm (equivalent to the energy-norm):

$$|||e|||^2 = (A\nabla e, \nabla e) = (A^{-1}e_\sigma, e_\sigma). \tag{4.14}$$

A recovered continuous flux $\sigma_h^* \in (S_h)^n$ is computed by smoothing the discontinuous over the elements numerical flux σ_h. The smoothing may be done by nodal averaging of σ_h, i.e. σ_h^* at a given node is computed by averaging the gradients σ_h at the elements that share the considered node, or $L^2(\Omega)$ projection of σ_h into $S_h \times S_h$. The computation of the global $L^2(\Omega)$-projection is expensive and one often uses "lumping" of the mass matrix to finally get

$$\sigma_h^*(P) = -\sum_{K\in\mathcal{T}_h} \frac{|K|}{|\Omega_P|} A\nabla u_h|_K,$$

where Ω_P is the union of elements sharing vertex P. Heuristically one may say that the continuous σ_h^* is better approximation to σ than σ_h. This justifies the idea to numerically evaluate (4.14) by taking $e_\sigma \approx \sigma_h^* - \sigma_h$. In [21] this heuristic approach has been theoretically studied for the finite element method for Poisson equation using regular triangular meshes. Next, we write $|||e|||^2 = \sum_{K\in\mathcal{T}_h} |||e|||_K^2$ and use the local quantity $\rho_K = |||e|||_K / |||u|||$ as an error indicator.

5. Adaptive grid refinement and solution strategy

In this section we present the used adaptive mesh refinement strategy. A brief general description follows. For a given finite element partitioning $\mathcal{T}_h$, desired error tolerance ρ and norm in which the tolerance to be achieved, say $|||\cdot|||$, do the following :

- compute the finite volume approximation $u_h \in S_h$, as given in Subsection 2.2;
- using the a posteriori error analysis compute the errors ρ_K for all $K \in \mathcal{T}_h$;

- mark those finite elements K for which $\rho_K \geq \rho/\sqrt{N}$; here N is the number of elements in $\mathcal{T}_h$;
- refine the marked elements;
- additionally refine until a conforming mesh is reached;
- repeat the above process until no elements have been marked.

The described procedure yields error control and optimal mesh (heuristics), which are the goals in any adaptive algorithm. The obtained in the process nested meshes are used to define multilevel preconditioners. The initial guess for every new level is taken to be the interpolation of u_h from the previous level. Concerning the solvers we also work on efficient preconditioning in parallel environment. More details about this can be found in our technical report [25].

For the 2-D case we refine marked elements by uniformly splitting the marked triangles into four. The refinement to conformity is done by bisection through the longest edge. For the 3-D version of the code the elements (tetrahedrons) are refined using the algorithm of Arnold, Mukherjee and Poly [3].

6. Numerical examples

6.1. **2-D model test problems.** We first present numerical experiments for the following model 2-D problems.

Example 1. We consider the problem (1.1) where Ω is an L-shaped domain given on Figure 4, $\Gamma_D \equiv \Gamma$, $\underline{b} = (1.5, 1)$, $f = 0$ and $A(x) = 0.01\ I$, where I is the identity matrix. The Dirichlet boundary values are 0 on $x = -1$ and $y = 1$, linearly increases from 0 to 1 on $(-1,-1)..(-1,-0.75)$ and 1 on the rest of the boundary. The up-wind scheme gives solution without oscillations. The local error estimators lead to local refinement around the expected boundary and internal layers. On Figure 4 we give the mesh on level 5 (left) which has $5,232$ nodes and $10,247$ triangles. On the right are the level curves of the solution computed on the same level.

Example 2. Again Ω is an L-shaped domain, $\Gamma_D \equiv \Gamma$, $\underline{b} = (1.5, 1)$ and $A(x) = 0.01\ I$. The Dirichlet boundary value is 0 everywhere. f is 0 everywhere except in the square with lower left and upper right corners $(-0.55, -0.55)$ and $(-0.45, -0.45)$ correspondingly. Figure 5 gives the mesh obtained after 4 level of refinement. It has $3,450$ nodes and $6,798$ triangles. On the right are the level curves of the solution.

Example 3. We take Ω to be the domain shown on Figure 6 with one internal layer. In this problem Γ_D is the upper boundary, $\underline{b} = (1, -0.5)$, $f = 0$ and $A(x) = 0.05\ I$ in the layer and $A(x) = 0.01\ I$ in the rest of the domain. The Dirichlet boundary value is 1 for $x < 0.2$ and 0 otherwise. On the Neumann boundary we take $g_N = 0$. Figure 6 shows the mesh on level 5 (left) with $6,035$ nodes and $11,892$ triangles. On the right are the solution level curves.

6.2. **3-D problems.** Next, we consider a problem related to simulation of steady state fluid flow, transport, and absorption of passive chemicals in porous media. The nonhomogeneous pressure of the aquifer will force the ground water to move and transport

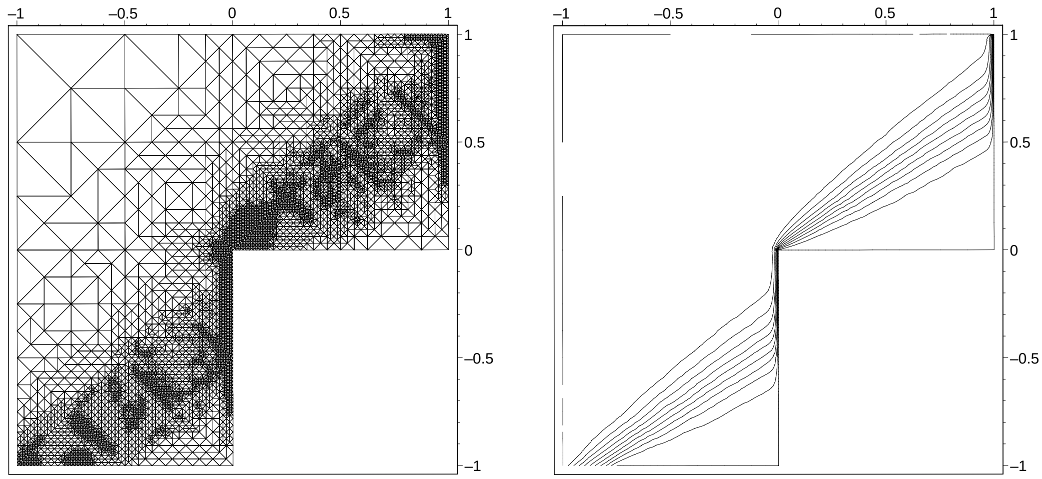

FIGURE 4. Convection dominant problem in L-shaped domain; the mesh on level 5 (left) with $5,232$ nodes and $10,247$ triangles; the level curves (right) on the same level.

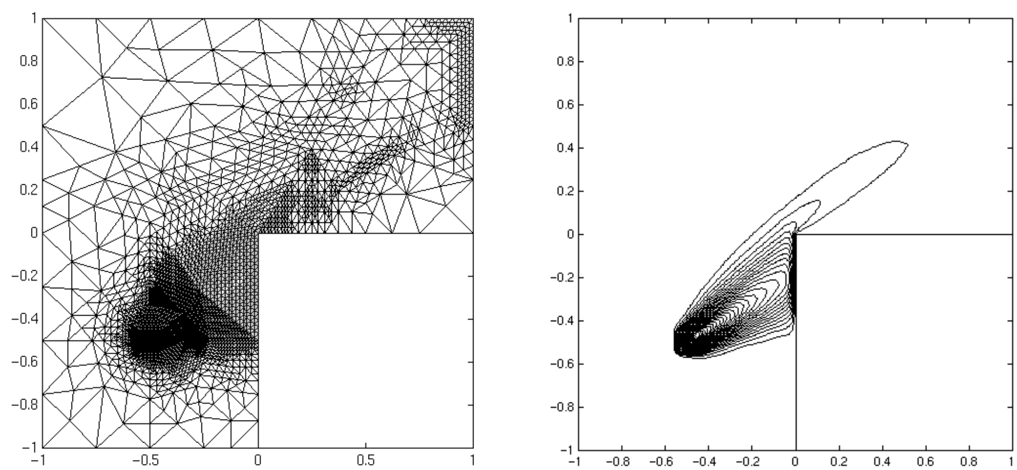

FIGURE 5. Convection dominant problem in L-shaped domain; the mesh on level 4 (left) with $3,450$ nodes and $6,798$ triangles; the level curves (right) on the same level.

the dissolved chemicals. Thus, we need to solve consecutively the pressure equation and the transport equation (diffusion-dispersion-reaction type).

We first consider the pressure equation with known solution in an L-shaped 3-D domain shown on Figure 7. Here $-1 < z < 1$. In this case $A(x) = I$, $f = 0$ and *Dirichlet* boundary $\Gamma_D = \partial\Omega \setminus \Gamma_N$, where $\Gamma_N = \{z = -1, 1\}$. This example has known exact solution $u(r, \theta, z) = r^{2/3} sin\frac{2\theta}{3}$ (in cylindrical coordinates) and has been used to test the error estimator.

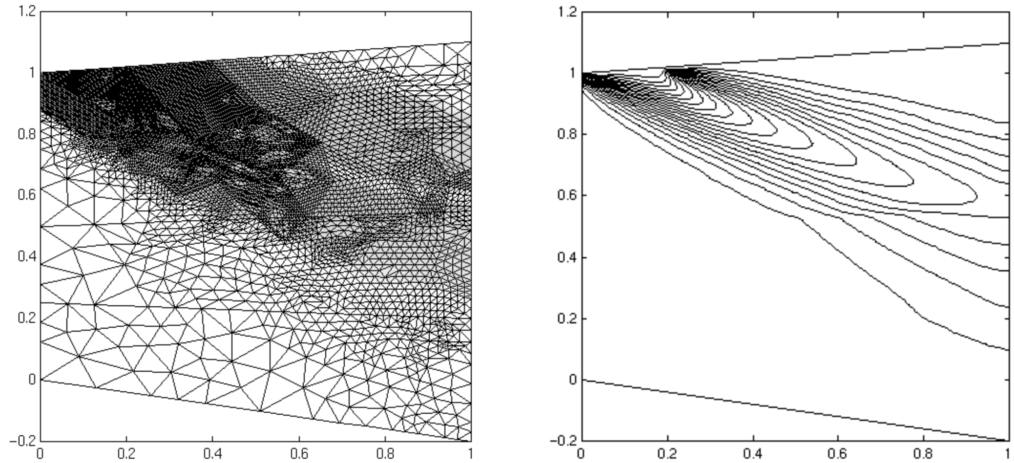

FIGURE 6. Convection dominant problem in domain with layers; the obtained locally refined mesh after 5 level of refinement (left) with 6,035 nodes and 11,892 triangles; the level curves (right) on the same level.

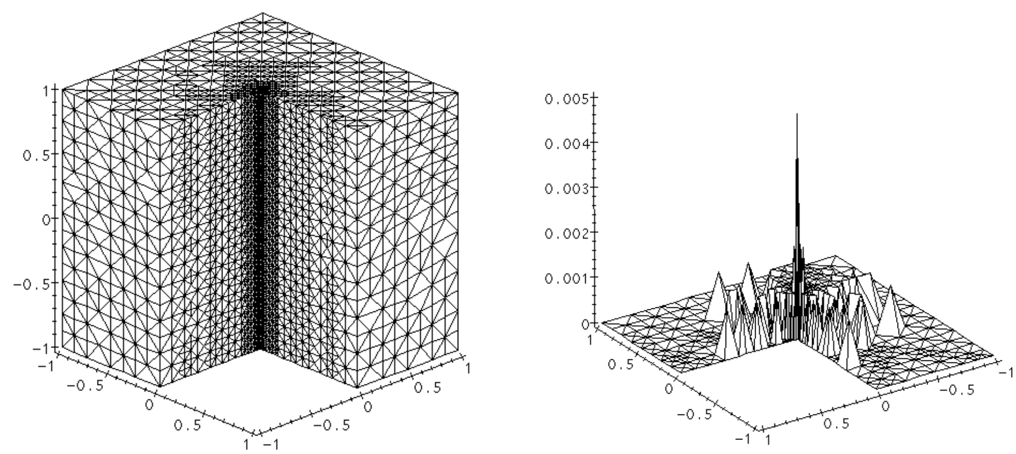

FIGURE 7. Poisson equation in L-shaped domain with solution given in cylindrical coordinates by $u(r,\theta,z) = r^{2/3} sin\frac{2\theta}{3}$, computed by ZZ refinement; the 3-D Mesh on level 6 (left) with 28,768 nodes, the mesh (middle) and error (right) for $z = 0$.

We have singularity along the edge with end points $(0,0,-1)$ and $(0,0,1)$. As expected the mesh shown on Figure 7 is repeatedly refined near this edge. On Figure 7 we show the 3-D mesh (left) on the sixth refinement level (see also Table 1) and the error (right) at a cross-section $z = 0.5$ (again on level six). Table 1 gives the results for the mesh and the error for the different levels of refinement obtained using ZZ local estimator. Error tolerance of 2% in the energy norm was imposed and obtained on level 6. Indeed, the energy norm of the exact solution is approximately $\sqrt{\pi/8} \approx 0.627$,

level	# nodes	$\|\|e\|\|_{max}$	$\|\|e\|\|_{L^2}$	$\|\|e\|\|_a$
1	509	0.050494	0.028660	0.123884
2	2,420	0.034936	0.010644	0.078138
3	8,813	0.022735	0.004112	0.049559
4	17,312	0.014491	0.001757	0.033087
5	22,448	0.009164	0.001048	0.024555
6	28,768	0.005807	0.000850	0.020348

TABLE 1. Local Refinement

level	# nodes	$\|\|e\|\|_{max}$	$\|\|e\|\|_{L^2}$	$\|\|e\|\|_a$
1	509	0.050494	0.028660	0.123884
2	3,333	0.034952	0.010643	0.077947
3	23,817	0.022750	0.004073	0.048743
4	179,729	0.014511	0.001586	0.030489
5	1,395,745	0.009186	0.000625	0.019107

TABLE 2. Uniform Refinement

i.e. on the last level we have approximately 3% error in the energy norm. The errors on the last level in the discrete L^2- and *maximum* norms are correspondingly 0.06% and 0.46%.

In order to compare with the case when no local refinement is applied we have included computations shown on Table 2 with *uniform* refinement. Here by *uniform* we mean that every tetrahedron has been split into 8. The accuracy with 1 395 745 nodes on level 5 is comparable to the accuracy of the locally refined grid with 28 768 nodes on level 6. Note, that the locally refined grid has about forthy times less grid points than the uniform grid.

We would like to mention that the other error indicators give similar results with small differences in the obtained meshes. However, the meshes are refined in the areas where the solution has some type of singularity and have almost the same number of nodes.

The last problem is based on data related to groundwater flow and the setting is described in below. A steady state flow, with Darcy velocity $\underline{v}$ (measured in *ft/yr*), has been established in a parallelepiped shaped reservoir of size $1000 \times 1000 \times 500$. The pressure $p(x)$ is a solution to the problem (1.1), where $\underline{b} \equiv 0$, $c \equiv 0$ and $A = D$, where D is the permeability tensor. The pressure at the the faces $x_1 = 0$ and $x_1 = 1000$ is constant, correspondingly 1000 and 0, the rest of the boundary is subject to no-flow condition, and the permeability tensor is $D = 64\ I$. In the layer (seen on Figures 8 and 9) we take the permeability to be five times smaller than in the rest of the domain, i.e. in the layer $D = 12.8\ I$. Finally, we have two wells with axes along the segments

$x_1 = 200$, $x_2 = 0$, $x_3 = 0..400$ and $x_1 = 400$, $x_2 = 0$, $x_3 = 0..400$. We treat the well simply as a line-delta function (sink) along the well axis. The production rate $Q = 200,000\ l/yr$ is the intensity of the sink. For discussion of various well boundary conditions we refer to [23].

On Figure 8 we show the adapted mesh and the level curves for the pressure in the reservoir cross-section $x_2 = 0$. The problem setting (see below) gives us symmetry with respect to the plane $x_2 = 0$, so the equations are solved only in half of the domain, the parallelepiped $(0, 1000) \times (0, 500) \times (0, 500)$.

The computed pressure p forces the ground water to flow with Darcy velocity $\underline{v} = -D\nabla p$. The transport of a contaminant, in our case benzene, dissolved in the water is described by the convection-diffusion-reaction equation (1.1), where u is the benzene concentration, $\underline{b}$ is the Darcy velocity $-D\nabla p$, $A(x)$ is the diffusion-dispersion tensor, and c is the biodegradation rate.

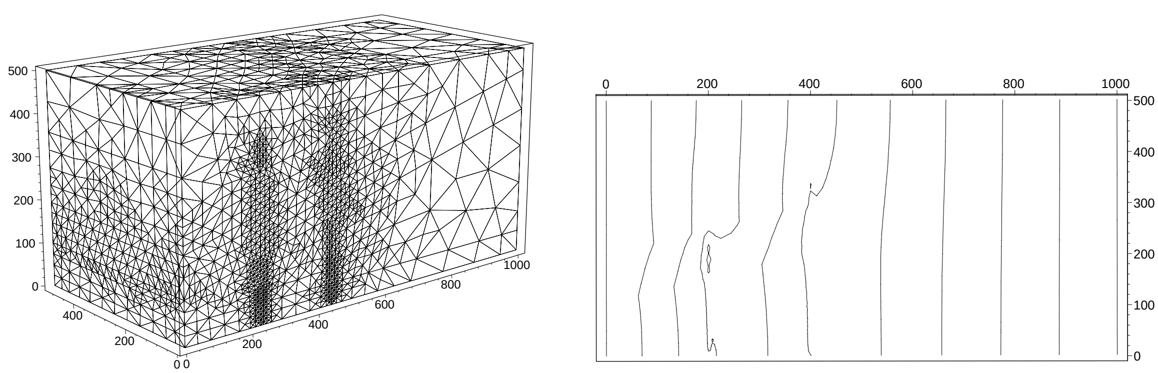

FIGURE 8. Pressure computations for a non-homogeneous reservoir with two wells; The two wells are in the plane $y = 0$; (left) the locally refined 3-D Mesh on level 3 with 16,705 nodes; (right) Contour curves of the pressure for level 3 in the plane $y = 0$

After the pressure is found with prescribed accuracy we use it to compute the Darcy velocity $\underline{v} = -D\nabla p$ and take $\underline{b} = \underline{v}$. The dispersion tensor A is given by $A(x) = k_{diff} I + k_t \underline{v}^T \underline{v}/|\underline{v}| + k_l(|\underline{v}|^2 I - \underline{v}^T \underline{v})/|\underline{v}|$, where $k_{diff} = 0.0001$, $k_t = 21$ and $k_l = 2.1$. A steady-state leakage of benzene of 30 mg/l is applied on the boundary strip $x_1 = 0$,x_3+50..350. The rest of the boundary is subject to homogeneous Neumann boundary condition. The wells have the given above production rate Q. The dispersion/convection process causes the dissolved benzene to disperse in the reservoir. The biodegradation is transforming the pollutant into a solid substance which is absorbed by the soil. This leads to a decrease in the benzene. The computations are for the case of low biodegradation rate

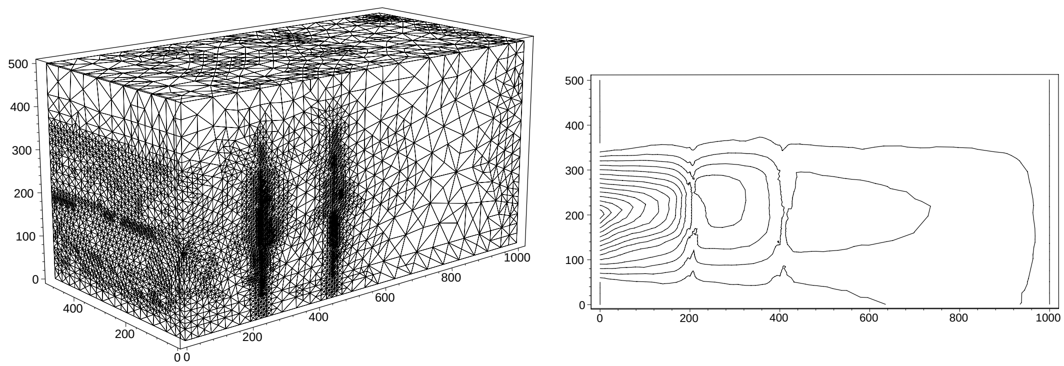

FIGURE 9. Concentration computations for a non-homogeneous reservoir; (left) the 3-D mesh on refinement level 5 with $44,980$ nodes; (right) contour curves of the concentration for the cross-section $x_2 = 0$; the permeability in the layer is two times smaller than the rest of the domain

$c = 0.05$. Figure 9 shows the obtained mesh and the isolines for the concentration in the reservoir cross-section $x_2 = 0$ on grid refinement level 5.

REFERENCES

[1] L. ANGERMANN, *Balanced a posteriori error estimates for finite-volume type discretizations of convection-dominated elliptic problems*, Computing, 55(4) (1995), pp. 305–324.

[2] L. ANGERMANN, *An a-posteriori estimation for the solution of an elliptic singularly perturbed problem*, IMA J. Numer. Anal., 12 (1992), pp. 201–215.

[3] D.N. ARNOLD, A. MUKHERJEE, AND L. POULY, *Locally adapted tetrahedral meshes using bisection*, SIAM J. Sci. Computing, 22(2) (2000), pp. 431–448.

[4] I. BABUSKA AND W.C. RHEINBOLDT, *Error estimates for adaptive finite element computations*, SIAM J. Numer. Anal., 15 (1978), pp. 736–754.

[5] R.E. BANK AND R.K. SMITH, *A posteriori error estimates based on hierarchical bases*, SIAM J. Numer. Anal., 30 (1993), pp. 921–932.

[6] R. BECKER AND R. RANNACHER, *A feed-back approach to error control in finite element methods: Basic analysis and examples*, East-West J. Numer. Math. 4(4) (1996), pp. 237–264.

[7] R. BECKER, C. JOHNSON, AND R. RANNACHER, *Adaptive error control for multigrid finite element methods*, Computing, 55(4) (1995), pp. 271–288.

[8] J.H. BRAMBLE, J.E. PASCIAK, AND O. STEINBACH, *On the stability of the L^2-projection on $H^1(\Omega)$,* Math. Comp., 70 (2001).

[9] S.C. BRENNER AND L.R. SCOTT, *The Mathematical Theory of Finite Element Methods*, Springer, 1996.

[10] Z. CAI, *On the finite volume element method,* Numer. Math., 58 (1991), pp. 713–735.

[11] Z. CAI, J. MANDEL, AND S. MCCORMICK, *The finite volume element method for diffusion equations on general triangulations,* SIAM J. Numer. Anal., 38 (1991), pp. 392–402.

[12] C. CARSTENSEN, *Quasi-interpolation and a posteriori error analysis in finite element methods,* Math. Model. Numer. Anal. M2AN, 33 (1999), pp. 1187–1202

[13] P. Clément, *Approximation by finite element functions using local regularization,* RAIRO Anal. Numer., 9 (1975), pp. 77–85.
[14] K. Eriksson, D. Estep, P. Hansbo, C. Johnson, *Computational Differential Equations*, Cambridge University Press, 1996.
[15] K. Eriksson and C. Johnson, *An Adaptive Finite Element Method for Linear Elliptic Problems*, Math. Comp., 50 (1988), pp. 361–382.
[16] R.E. Ewing, R.D. Lazarov and Y. Lin, *Finite volume element approximations for nonlocal reactive flows in porous media*, Numer. Meth. PDE's, 16(3) (2000), pp. 285–311.
[17] T. Ikeda, *Maximum Principle in Finite Element Models for Convection-Diffusion Phenomena*, Lecture Notes in Numer. Appl. Anal., **4** (1983), North-Holland, Amsterdam New York Oxford.
[18] R.D. Lazarov, J.E. Pasciak and S.Z. Tomov, *Error control, local grid refinement and efficient solution algorithms for singularly perturbed problems*, Analytical and Numerical Methods for Convection-Dominated and Singularly Perturbed Problems (L.G. Vulkov, J.J.H. Miller, and G.I. Shishkin, Eds), NOVA Science Publ. Inc., 2000, pp. 71–82.
[19] R.H. Li and Z.Y. Chen, *The Generalized Difference Method for Differential Equations*, Jilin University Publishing House, 1994.
[20] I.D. Mishev, *Finite volume methods on Voronoi meshes*, Numer. Methods for Partial Differential Equations, 14 (1998), pp. 193–212.
[21] R. Rodriguez, *Some remarks on Zienkiewicz-Zhu estimator*, Numer. Methods for Partial Differential Equations, 10 (1994), pp. 625–635.
[22] H.-O. Ross, M. Stynes, and L. Tobiska, *Numerical Methods for Singularly Perturbed Differential Equations*, Springer, 1996.
[23] M. Slodicka and R. Van Keer, *A nonlinear elliptic equation with non-local boundary condition solved by linearization*, Dept. of Mathematics, University of Gent, Belgium, Preprint 1, (2000).
[24] M. Tabata, *A finite element approximation corresponding to the upwind finite differencing*, Mem. Numer. Math., 4 (1977), pp. 47–63.
[25] S. Z. Tomov, *Tool-box for large scale parallel simulation of* 3*-D flow and transport in porous media*, Texas A&M University, TAMU, ISC Technical Reprt, ISC-01-06-MATH, 2001.
[26] R. Verfürth, *A Review of a Posteriori Error Estimators and Adaptive Mesh Refinement Techniques*, Teubner-Wiley, Stuttgart, 1996.
[27] R. Verfürth, *A posteriori error estimation and adaptive mesh-refinement techniques*, J. Comp. Appl. Math., 50 (1994), pp. 67–83.
[28] J. Xu and L. Zikatanov, *A monotone finite element scheme for convection-diffusion equations*, Math. Comp., 68 (1999), pp. 1429–1447.
[29] O.C. Zienkiewicz and J.Z. Zhu, *A Simple Error Estimator and Adaptive Procedure for Practical Engineering Analysis*, Int. J. Numer. Meth. Engng., 24 (1987), pp. 337–357.
[30] O.C. Zienkiewicz and J.Z. Zhu, *Adaptivity and mesh generation*, Int. J. Numer. Mrthods Engrg. 32 (1991).

Department of Mathematics, Texas A&M University, College Station, TX 77843-3368
E-mail address: lazarov@math.tamu.edu

Department of Mathematics, Texas A&M University, College Station, TX 77843-3404
E-mail address: tomov@math.tamu.edu